

# Covariances and parameter confidence intervals from light-element R-matrix evaluations

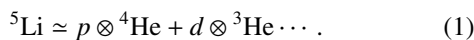
Mark Paris<sup>1,\*</sup> and Gerald Hale<sup>1,\*\*</sup>

<sup>1</sup>Theoretical Division, Los Alamos National Laboratory, MS B283, Los Alamos, New Mexico 87545

**Abstract.** R-matrix parameter covariances for light elements with  $A \leq 16$  are calculated within the Wigner-Eisenbud multichannel unitary R-matrix theory. We review the theoretical foundation, numerical approach, and determination of the parameter covariances within this approach. We derive the relation between the parameter variance, as the diagonal elements of the covariance matrix, and the parameter confidence interval based upon the chi-squared distribution. Cross section covariances computed from the parameter confidence intervals are calculated for several compound systems and discussed.

## 1 Introduction

Nuclear reaction and scattering cross section information continues to be an indispensable component in design, modeling, simulation and refinement of complex systems in nuclear science, energy, and security. The ability to assess the validity of modeling and simulation capabilities, in particular, depends on the characterization and quantification of uncertainty associated with nuclear reaction and scattering observables. We should emphasize that we are not just referring to the energy-dependent, angle-integrated cross sections  $\sigma(E)$ , but the full, complete set of observables that comprise those associated with a particular compound system  $^A\mathcal{Z}$  that couples to all of the two- (and more) body partitions. For example, for the compound system of  $^5\text{Li}$ , relevant two body partitions in order of increasing total partition mass, are



The observables for this system are the set of total, angle-integrated, and angular distributions of both unpolarized (spin-independent) and polarized or spin-dependent versions of these quantities. The advantage of being able to handle all of these types differential data has been discussed in Ref.[1]. These observables may be formed from the initial state spin density matrix elements  $\rho^{(i)}$  and the transition  $T$  matrices for reactions and scattering (where the final partition composed of the same nuclides as the initial partition, but the masses may differ for inelastic scattering) as

$$\rho^{(f)} = T \rho^{(i)} T^\dagger. \quad (2)$$

This spin-density matrix approach, which follows closely along the lines of Ref.[2], constitutes a general methodology for computing model representations and confers a

smooth (differentiable) representation of reaction and scattering data for general compound system.

Our focus in this present work is on light  $A \leq 20$  systems; the R-matrix formalism is discussed in some detail in Ref.[1]. Observed data for all processes (total, elastic and reactions for both unpolarized and polarized data) is fit via least squares, the topic of the next section, Sec.2. The determination of the covariances from such a fit is the main focus of the present work. In section 3, we apply the method to the several compound systems. Conclusions are given in Sec.4.

## 2 Least squares fitting and covariance determination

Least squares fitting is accomplished via the R-matrix approach to reaction theory. The  $\chi^2$  function is formed as a sum over the included data for all experiments of processes that couple to a particular compound system. The general expression for the  $\chi^2$  function, which may be regarded as a log-likelihood function, is given as:

$$\chi_{EDA}^2(p, n_M) = \sum_{M, i_M} \left[ \frac{n_M X_{i_M}(p) - R_{i_M}}{\Delta R_{i_M}} \right]^2 + \left[ \frac{n_M S_M - 1}{\Delta S_M / S_M} \right]^2. \quad (3)$$

The sum is over the measurement setups  $M$  or different experiments. Each experiment  $M$  is comprised of kinematical points and observable values denoted  $R_{i_M}$ , indexed by  $i_M$ . Predictions  $X_{i_M}(p)$  are given generally as ratios of the elements of the spin-density matrix and their sums (such as the trace for the unpolarized angular distributions) and expressed as functions of the variational parameters  $p_\alpha$ , which are  $N_p$  in number. Normalization factors  $n_M$  are varied for either relative or absolute measurements. In the case of relative measurements, the experimental normalization is chosen to eliminate the second term in the

\*e-mail: mparis@lanl.gov

\*\*e-mail: ghale@lanl.gov

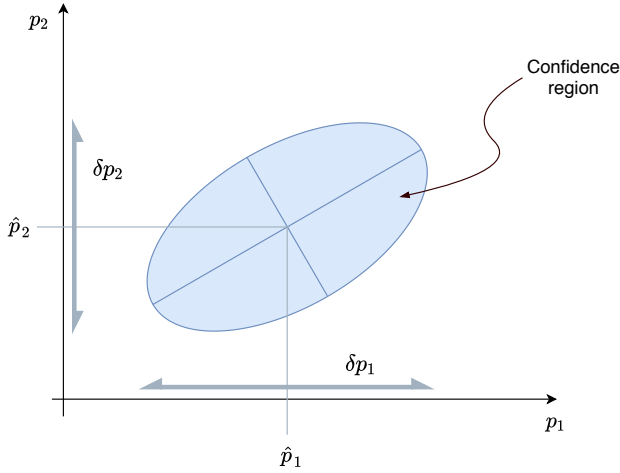


**Figure 1.** Confidence ellipse determined near the minimum of the function  $\chi^2_{EDA}(\hat{p})$ .

above equation [eq. (3)]. Absolute measurement normalizations are allowed to vary in accordance with either the quoted experimental normalization uncertainty  $\Delta S_M$  or, if this uncertainty is underdetermined, by an assumed amount deemed to be reasonable, sometimes as large as a few 10's of percent but usually  $< 10\%$ .

The above form for  $\chi^2_{EDA}(p, n_M)$  should be compared to a *standard* form[3], which takes into account data covariance through the elements of a matrix  $V_{ij}$  as

$$\chi^2(p) = \sum_{ij} (X_i(p) - A_i) V_{ij}^{-1} (X_j(p) - A_j), \quad (4)$$

in a simplified notation that keeps the experimental setup index  $M$  implied. (We also drop explicit reference to the normalizations,  $n_M$ , which may be considered to present.) Here absolute measurements are defined as  $A_i = R_{iM} S_M$ , where the observable  $R_{iM}$  and the experimental normalization  $S_M$  are defined above. The form  $\chi^2_{EDA}(p)$  is recovered in the limit that the data covariance matrix has the form

$$\text{cov}(R_i, R_j) = \delta_{ij} (\delta R_i)^2, \quad (5)$$

$$\text{cov}(S_i, S_j) = \delta_{ij} (\delta S_i)^2, \quad (6)$$

$$\text{cov}(R_i, S_j) = 0. \quad (7)$$

### 2.0.1 Parameter uncertainty scaling

The determination of uncertainties in the parameter values is given by the usual analysis[4] at a local (assumed to be global) minimum of the function  $\chi^2_{EDA}(p)$  given by parameter values  $p = \hat{p}$ . About this minimum, the function  $\chi^2_{EDA}(p)$  assumes the quadratic form

$$\delta\chi^2_{EDA}(p) \equiv \chi^2_{EDA}(p) - \chi^2_{EDA}(\hat{p}) = \delta p_\alpha C_{\alpha\beta}^{-1} \delta p_\beta, \quad (8)$$

where  $\delta p_\alpha \equiv p_\alpha - p_{0,\alpha}$  and  $C$  is the parameter covariance matrix (the summation convention on repeated indices is implied). The standard analysis, given in Arndt

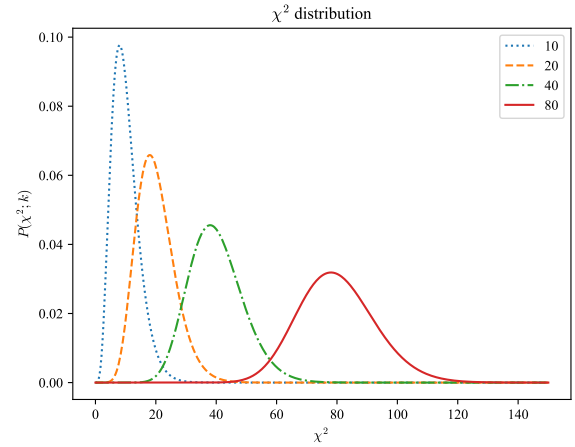


**Figure 2.** The  $\chi^2$  distribution for  $k$  degrees of freedom.

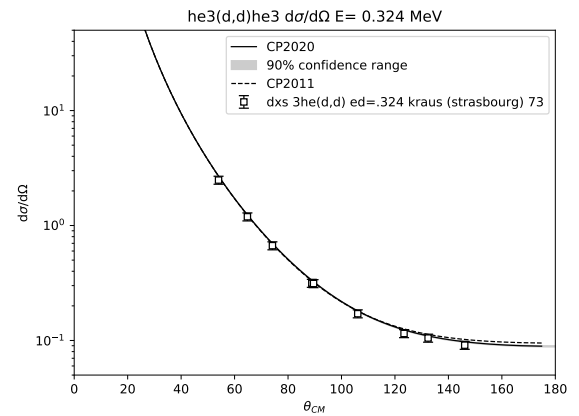


**Figure 3.** The angular distribution for  ${}^3\text{He}(d, d){}^3\text{He}$  for deuteron incident laboratory energy 324 keV of the unpolarized differential cross section in the center of mass as a function of the center of mass angle  $\theta_{cm}$ . The evaluation is shown by the solid curve. The gray band is the 90% confidence interval determined as described in the text.

and MacGregor[4], at this local minimum, which considers the marginalization of a single parameter  $p_\alpha$ , gives the uncertainty in terms of the change of the  $\chi^2$  function and the diagonal covariance element (the variance)  $C_{\alpha\alpha}$  as

$$(\delta p_\alpha)^2 = \delta\chi^2 C_{\alpha\alpha}. \quad (9)$$

Choosing  $\delta\chi^2$  in the usual manner,  $\delta\chi^2 \equiv 1$  however, leads to the following scaling behavior with  $N_p$ , the number of fit parameters:

$$\delta p_\alpha = (C_{\alpha\alpha})^{1/2} \sim \mathcal{O}(N_p^{-1/2}), \quad (10)$$

as can readily be seen in fig. 1; fixing the  $\chi^2$  hypersurface as  $\delta\chi^2 = 1$  results in the scaling relation above. This scaling behavior results in the uncomfortable situation that adding marginal or redundant parameters lowers the uncertainty of all the parameters.

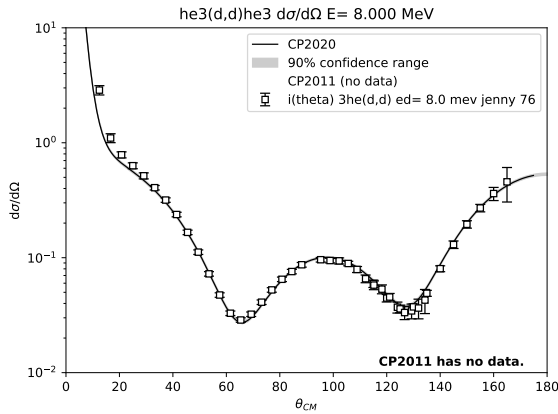
An improvement in the scaling behavior in eq. (10) is obtained if we choose a measure of the  $\chi^2$  hypersur-

Channel	$a_c$ (fm)	$\ell_{max}$
$d + {}^3\text{He}(\frac{1}{2}^+)$	4.8	4
$p + {}^4\text{He}(0^+)$	2.9	4
$p + {}^4\text{He}^*(0^+; 20.2 \text{ MeV})$	3.4	2
$d_0 + {}^3\text{He}(\frac{1}{2}^+)$	5.1	0

Reaction	Energy Range (MeV)	# Data Points	Observables
${}^3\text{He}(d, d){}^3\text{He}$	$E_d = 0.32 - 10.0$	2,229	$\sigma(\theta), A_i, A_{ii}, C_{i,j}, C_{ij,k}, K_{i,j'k'}, K_{ij,k'l'}$
${}^3\text{He}(d, p){}^4\text{He}$	$E_d = 0.13 - 10.0$	3,839	$\sigma(E), \sigma(\theta), A_i, A_{ii}, C_{i,j}, K_{ij,k'}$
${}^3\text{He}(d, p){}^4\text{He}^*$	$E_d = 3.70 - 6.70$	28	$\sigma(\theta)$
${}^4\text{He}(p, p){}^4\text{He}$	$E_p = 0.92 - 34.3$	867	$\sigma(E), \sigma(\theta), A_y, P_y$
Total:		6963	

**Table 1.** Channel configuration (top) and data summary (bottom) for the  ${}^5\text{Li}$  system analysis. The column labeled “Observables” indicates the following data types:  $\sigma(E)$ , integrated cross section;  $\sigma(\theta)$ , unpolarized angular distributions (energy-dependence suppressed);  $A$  initial-state analyzing power;  $P$  final-state polarization;  $C$  spin correlation coefficients;  $K$  polarization transfer coefficients. (We have suppressed the indices  $i, j, \dots$  which take on values  $x, y, z$  for spins/polarization directions in configuration space.) All polarization and spin distributions are angular distributions, which depend on the angle of the outgoing particle. Chi-squared per degree of freedom for the analysis is  $\chi^2/\text{dof} \approx 2.7$  over 7,178 data points, 215 of which were discarded by eliminating individual data points which contribute to  $\chi^2 > 40$ .



**Figure 4.** The angular distribution for  ${}^3\text{He}(d, d){}^3\text{He}$  for deuteron incident laboratory energy 8.0 MeV of the unpolarized differential cross section in the center of mass as a function of the center of mass angle  $\theta_{cm}$ . The evaluation is shown by the solid curve. The gray band is the 90% confidence interval determined as described in the text.

face that depends on the number of parameters  $N_p$ . Following Ref.[5], we recognize that, given the fact that the  $\chi^2$ -function is a statistic distributed according to the  $\chi^2$ -distribution. A detailed analysis[5] supports this observation and we arrive at a description of the parameter uncertainty in terms of the confidence interval, chosen as the upper limit of the cumulative  $\chi^2$  distribution function  $P(\delta\chi^2; k)$  for  $k$  degrees of freedom as:

$$P(\delta\chi^2; k) = (2^{k/2}\Gamma(k/2))^{-1} \int_0^{\delta\chi^2} dt t^{k/2-1} e^{-t/2}, \quad (11)$$

which is shown in fig. 2. Given that the mode and average of the  $\chi^2$  distribution are  $k - 2$  and  $k$ , respectively, we

estimate using eq. (9), the scaling of the uncertainty of  $p_\alpha$  to be

$$\delta p_\alpha \sim N_p^{1/2} C_{\alpha\alpha}^{1/2}. \quad (12)$$

The above analysis has been applied to the  ${}^5\text{Li}$  compound system. The  $R$ -matrix configuration for this system is shown in the table.

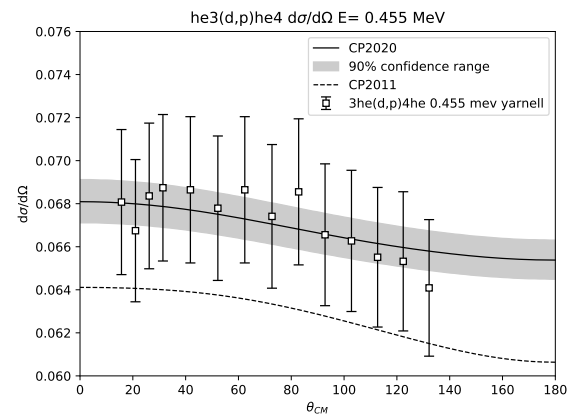


**Figure 5.** The angular distribution for  ${}^3\text{He}(d, p){}^4\text{He}$  for deuteron incident laboratory energy 455 keV of the unpolarized differential cross section in the center of mass as a function of the center of mass angle  $\theta_{cm}$ . The evaluation is shown by the solid curve. The gray band is the 90% confidence interval determined as described in the text.

### 3 Application to ${}^5\text{Li}$ compound system

We have applied the uncertainty quantification in terms of parameter confidence intervals described above to the  ${}^5\text{Li}$

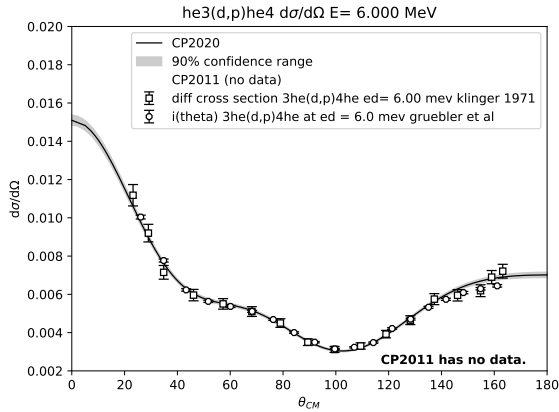


**Figure 6.** The angular distribution for  ${}^3\text{He}(d, p){}^4\text{He}$  for deuteron incident laboratory energy 6.0 MeV of the unpolarized differential cross section in the center of mass as a function of the center of mass angle  $\theta_{cm}$ . The evaluation is shown by the solid curve. The gray band is the 90% confidence interval determined as described in the text.

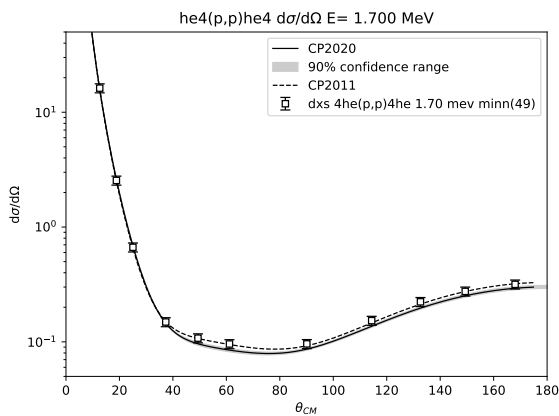


**Figure 7.** The angular distribution for  ${}^4\text{He}(p, p){}^4\text{He}$  for deuteron incident laboratory energy 1.7 MeV of the unpolarized differential cross section in the center of mass as a function of the center of mass angle  $\theta_{cm}$ . The evaluation is shown by the solid curve. The gray band is the 90% confidence interval determined as described in the text.

compound system. The  $R$ -matrix configuration is shown in table 1. The two-particle partitions include the ground-state  ${}^3\text{He}$  component,  $d + {}^3\text{He}(\frac{1}{2}^+)$ ,  $p + {}^4\text{He}(0^+)$  – the proton  ${}^4\text{He}$  ground-state component, its first excited state  $p + {}^4\text{He}^*(0^+; 20.2 \text{ MeV})$ , and the scalar-isovector partner of the two-nucleon virtual bound state,  $d_0 + {}^3\text{He}(\frac{1}{2}^+)$ . These are shown in the upper part of table 1, along with the channel radius  $a_c$  and the maximum value of the partition orbital angular momentum,  $\ell_{max}$ . The fit data – processes (elastic, reaction, . . . ), energy range, number and types of data – included in the  ${}^5\text{Li}$  system evaluation is shown in the bottom table.

At the solution, set by an upper limit on the size of the gradient of 1 part in  $10^6$ , we determine the parameter uncertainties as described in the previous section and propagate

their error according to standard error propagation via the “sandwich” rule; see Ref.[1]. A few examples (out of hundreds generated by fitting the  $\sim 7k$  data points for the  ${}^5\text{Li}$  system) are shown in figs. 3 to 8. Figures 3 and 4 show the elastic scattering of  $d$  from  ${}^3\text{He}$  for a deuteron laboratory energy of 324 keV. Curves are shown in fig. 3 for a more recent evaluation (CP2020, which will be included in the ENDF/B-VIII.1 release in 2024) and the older evaluation (CP2011, which is equivalent to ENDF/B-VIII.0[6]) plotted against the data by Ref.[7]. Figure 4 shows data similar to the previous figure, plotted against the data from Ref.[8]. The  $(d, p)$  reaction data is shown in figs. 5 and 6 and finally the proton elastic data is displayed in figs. 7 and 8.

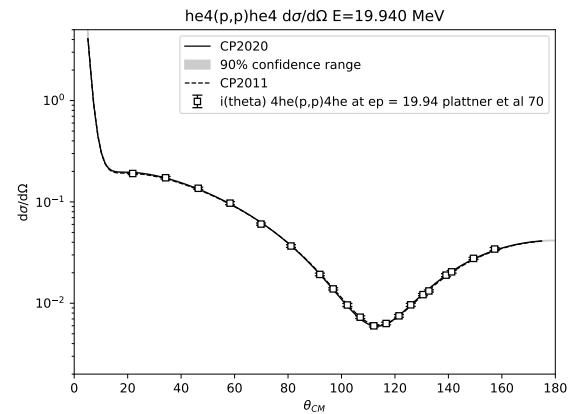


**Figure 8.** The angular distribution for  ${}^4\text{He}(p, p){}^4\text{He}$  for deuteron incident laboratory energy 19.94 MeV of the unpolarized differential cross section in the center of mass as a function of the center of mass angle  $\theta_{cm}$ . The evaluation is shown by the solid curve. The gray band is the 90% confidence interval determined as described in the text.

## 4 Conclusions

Confidence intervals for  $R$ -matrix evaluations have been determined from the  $\chi^2$  distribution. We have motivated an improvement in the scaling of the parameter uncertainties with the number of parameters  $N_p$  in the fit. We applied this methodology to the  ${}^5\text{Li}$  compound system in an evaluation of  $\sim 7k$  differential and integral data points. The improved scaling of the parameter uncertainties resolves some long standing issues associated with  $R$ -matrix evaluations yielding cross section uncertainties that are too small[9].

## References

- [1] G. Hale, Nucl. Data Sheets **109**, 2812 (2008)
- [2] L. Wolfenstein, Annual Review of Nuclear Science **6**, 43 (1956)
- [3] D. Smith, *Probability, Statistics, and Data Uncertainties in Nuclear Science and Technology*, Monograph Series (American Nuclear Society, 1991), ISBN 9780894480362

- [4] R.A. Arndt, M.H. MacGregor, *Methods in Computational Physics* **6**, 253 (1966)
- [5] Y. Avni, *Astrophys. Journ.* **210**, 642 (1976)
- [6] D. Brown et al., *Nucl. Data Sheets* **148**, 1 (2018)
- [7] L. Kraus (1971), PhD. Thesis
- [8] B. Jenny, W. Gruebler, V. Konig, P.A. Schmelzbach, R. Risler, H.R. Burgi, D.O. Boerma, *Nuclear Physics, Section A* **324**, 99 (1979)
- [9] A. Carlson et al., *Nucl. Data Sheets* **148**, 143 (2018)